JOURNAL OF THE ROYAL SOCIETY Interface

rsif.royalsocietypublishing.org

Research

Cite this article: Chen Y-K, Liao C-P, Tsai F-Y, Chi K-J. 2013 More than a safety line: jump-stabilizing silk of salticids. J R Soc Interface 10: 20130572.
http://dx.doi.org/10.1098/rsif.2013.0572

Received: 26 June 2013
Accepted: 17 July 2013

Subject Areas:
biomechanics, biomaterials, biophysics

Keywords:
jumping spiders, dragline silk, stability control, pitch reversal, biomechanics

Author for correspondence:
Kai-Jung Chi
e-mail: kjchi@phys.nchu.edu.tw

†Present address: School of Medicine, Taipei Medical University, Taipei 110, Taiwan.

Electronic supplementary material is available at http://dx.doi.org/10.1098/rsif.2013.0572 or via http://rsif.royalsocietypublishing.org.

Royal Society Publishing
Informing the science of the future

More than a safety line: jump-stabilizing silk of salticids

Yung-Kang Chen[1,†], Chen-Pan Liao[2,3], Feng-Yueh Tsai[3] and Kai-Jung Chi[3]

[1]National Taichung First Senior High School, Taichung 40403, Taiwan
[2]Department of Life Science, Tunghai University, Taichung 407, Taiwan
[3]Department of Physics and Institute of Biophysics, National Chung Hsing University, Taichung 40227, Taiwan

Salticids are diurnal hunters known for acute vision, remarkable predatory strategies and jumping ability. Like other jumpers, they strive for stability and smooth landings. Instead of using inertia from swinging appendages or aerodynamic forces by flapping wings as in other organisms, we show that salticids use a different mechanism for in-air stability by using dragline silk, which was previously believed to function solely as a safety line. Analyses from high-speed images of jumps by the salticid *Hasarius adansoni* demonstrate that despite being subject to rearward pitch at take-off, spiders with dragline silk can change body orientation in the air. Instantaneous drag and silk forces calculated from kinematic data further suggest a comparable contribution to deceleration and energy dissipation, and reveal that adjustments by the spider to the silk force can reverse its body pitch for a predictable and optimal landing. Without silk, upright-landing spiders would slip or even tumble, deferring completion of landing. Thus, for salticids, dragline silk is critical for dynamic stability and prey-capture efficiency. The dynamic functioning of dragline silk revealed in this study can advance the understanding of silk's physiological control over material properties and its significance to spider ecology and evolution, and also provide inspiration for future manoeuvrable robot designs.

1. Introduction

Many animals jump as a means of locomotion and to overcome obstacles or gaps, escape from danger, mount hosts or prey and launch into flight [1]. Jumping has been of biomechanical interest for many decades, particularly concerning energetics and take-off. Various mechanisms have evolved in jumpers to obtain sufficient kinetic energy for take-off or further destinations, including longer limbs with larger muscles, elastic energy storage and catapult mechanisms for rapid power output [2–6]. However, jumpers also face challenges to maintain in-air stability and smooth landing, because falling may lead to injury or extra energy costs in returning to the canopy. Besides adjusting the centre of mass (CoM) close to the vector of propulsive thrust at take-off to avoid later body rotation [7,8], some jumpers actively use dynamic control for in-air stability. Two mechanisms have previously been proposed to counteract unwanted torque in the air: using the inertia of swinging appendages [9–12] and aerodynamic forces from flapping wings [6,7]. Take-off mechanisms and stability control that evolved in nature have led to significant progress in bioinspired designs for manoeuvrable jumping robots [11,13].

Jumping spiders, members of the family Salticidae, are diurnal hunters known for their acute vision, remarkable predatory strategies and jumping ability [14–17]. They jump for prey capture, escape and rapid point-to-point movement. Before take-off, they attach dragline silk to the substrate, presumably as a safety line as proposed for orb-weaving spiders [14,18,19]. Unlike other arthropods, spiders have no extensor muscle in their major leg joints and use rapid increase of hydraulic pressure in the hind legs to launch a jump [14,20]. Parry & Brown reported an occasion of somersaulting after a

salticid's dragline silk was broken [21], implying silk's functioning towards motion control [22].

Dragline silk is widely used in spiders for various mechanical functions. Besides being a safety line (or lifeline) for unexpected falling and as a guide to return to the starting position [14,18,23], it is also used by spiders for locomotion (ballooning) [24], braking while jumping through air or fishing on water surfaces [21,22,25] and as a framework for web construction [14,19]. Ranked among the toughest materials known [26,27], spider silk has drawn substantial attention to the molecular basis for its remarkable properties and ultimately for its potential applications [28–30]. The dragline's outstanding tensile strength and toughness are important in its role as a safety line [19], whereas its unusual torsional properties may prevent an abseiling spider from swinging or rotating, a movement that might attract predators [31]. To serve as a useful safety line, new silk has to be produced during the spider's fall to prevent it from breaking [32]. Although rapid spinning might stiffen the silk and hence provide a greater resistant force, the falling spider most likely stops itself by using an internal friction brake [33], presumably the 'valve' of the spider's spinning system [34], that clamps onto the passing silk.

Most studies on spider (and even insect) jumping have focused on take-off mechanisms or overall jumping performance, but few have discussed body rotation and stability after take-off. Among jumpers, salticids are unique because they attach dragline silk to the substrate before take-off. Although dragline silk has been observed in braking and motion control during spider jumping [21,22], the dynamic functioning of dragline silk in spider locomotion remains less examined [32,33]. A thorough understanding of the natural uses of silk not only allows us to explore its significance in salticid biology but also provides biological inspiration for future manoeuvrable robot designs.

To examine the functioning mechanisms of dragline silk as an in-air stabilizer for spider jumping, we (i) analysed the motion of normal and non-silk salticids throughout jumps that were recorded using high-speed videography, (ii) estimated instantaneous silk force from kinematic data, (iii) associated body motion with the magnitude and direction of silk force, and (iv) summarized these findings in the context of silk's material properties and physiological control for silk production.

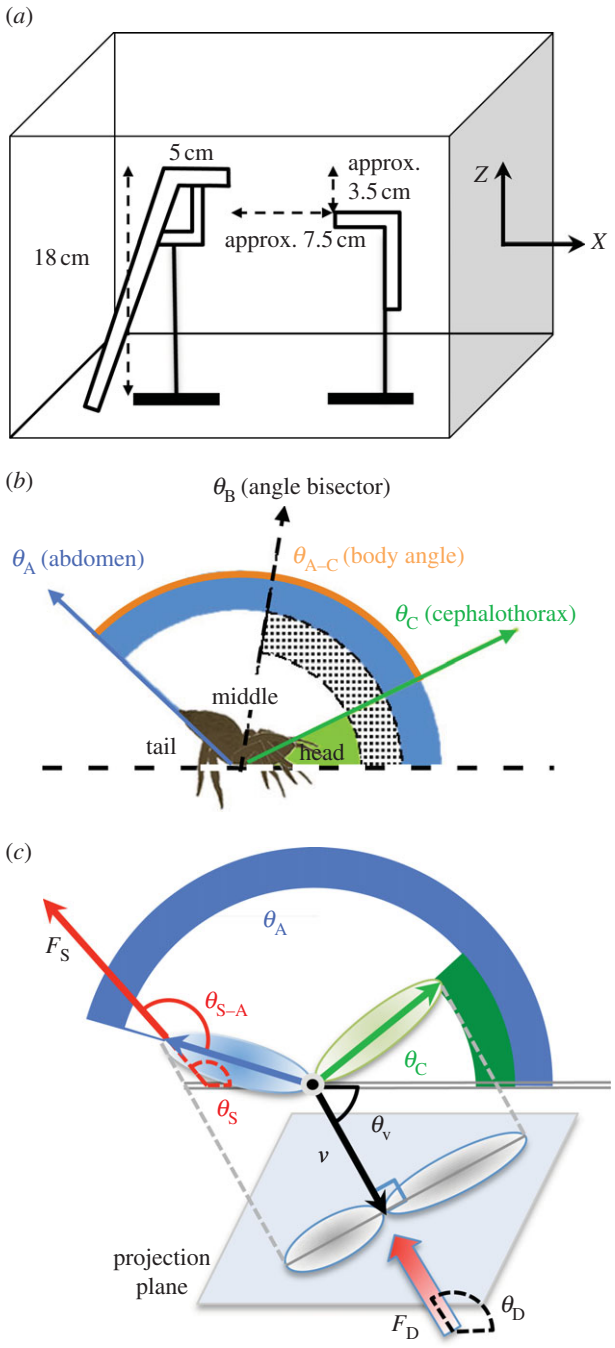

Figure 1. Schematic of the experimental set-up and mechanical analyses. (*a*) Take-off and landing platforms. (*b*) Body orientation depicted by the cephalothorax (θ_C), abdomen (θ_A) and body angles ($\theta_{A-C} = \theta_A - \theta_C$). The angle bisector ($\theta_B$) represents the mean body direction. (*c*) Free-body diagram of a salticid jumping at velocity (v) and subjected to drag (F_D) and silk forces (F_S), with directions θ_v, θ_D and θ_S, respectively. Drag acts in the opposite direction of velocity. The angle between the silk and the abdomen is θ_{S-A}. The area used for calculating drag is that which is projected onto a plane normal to the instantaneous velocity vector. Legs (not shown) have a surface area similar to that of the body.

2. Material and methods

2.1. Animals

We used 27 completely intact samples of Adanson's House Jumper (*Hasarius adansoni*) collected near Taichung City to study the role of silk during spider jumping. Spiders were kept individually in captivity at room temperature (21–24°C), supplied with water and fed with three or four fruitflies two or three times a week. Each subject underwent four experimental sessions during eight weeks of captivity. The first session commenced after a week of acclimation in the laboratory, with intervals between sessions being longer than a week. Among the subjects collected, five did not attach dragline silk at the take-off stage during the initial experimental session and remained non-silk throughout the whole experimental period, whereas the other 22 subjects consistently left dragline silk attached to the take-off stage during all experiments and to substrates during daily activity. Owing to the small size of these spiders, we were not successful in blocking the silk glands with wax to create experimentally manipulated non-silk spiders. Instead, we used the natural non-silk spiders as controls. There were no other observed differences in feeding or activity between the two groups. During the experiments, all subjects, normal and non-silk, were able to climb onto an elevated platform of height of 18 cm and jump onto a lower stage 7.5 cm away (figure 1*a*). The body mass (BM) of each subject was measured using a laboratory scale immediately after the experiments. Body length (BL) was measured from images as the sum

of cephalothorax and the abdominal lengths. The cephalothorax is typically used as a measure for BL because abdomen size can change considerably with physiological condition. But here, we report total length here as it affects the amount of drag as well as the silk's moment exerted on the body.

Although no differences were found in feeding and behaviour between the two groups, to assure that the non-silk condition did not affect jumping performance we compared body size and jumping ability of 15 normal and four non-silk subjects whose jumps were recorded successfully for kinematic analyses. Normal spiders had BMs of 19.95 ± 4.71 mg and BLs of 6.1 ± 0.3 mm ($n = 15$), and the non-silk spiders had BMs of 21.14 ± 2.83 mg and BLs of 6.0 ± 0.2 mm ($n = 4$; table 1). To compare body condition between silk and non-silk subjects, we conducted a one-way multivariate analysis of variance (MANOVA). Results suggest that the body size (BM, BL) was not significantly different between the two groups ($\Lambda_{\text{Wilks}} = 0.94865$, $F_{2,16} = 0.4330$, $p = 0.6559$; electronic supplementary material, figure S1). Jumping ability was assessed using take-off velocity (v_i; table 1) because it mechanically determines the distance of a jump. We examined whether the two groups had similar v_i values by fitting with a general linear mixed model (GLMM) where silk condition was set as a fixed factor (value of 1 for silk, 0 for non-silk), an individual was treated as a random factor nested within the silk condition, and BM and BL were assigned as covariates. Results suggest no significant difference in v_i between the two groups ($T_{17} = 0.9844$, $p = 0.3387$; electronic supplementary material, table S1). Because no observed differences in feeding, behaviour and physical condition were found between the two groups, the four abnormal non-silk producing subjects were otherwise considered normal and healthy for the purposes of this study.

2.2. Kinematics of spider jumping

In nature, salticids might jump to destinations of different heights and distances up to 25 times their own BL [14,22]. Here, we considered only subhorizontal jumps to a lower destination to simplify analyses. We designed and constructed a jumping platform with a narrow take-off stage (approx. 3×5 cm) at a height of 18 cm (figure 1*a*). Each subject was released at the stage bottom to climb up the slope to the take-off stage and jumped onto a destination within the salticids' 10 cm field of view [14]. Because the destination stage was the only obvious target within the covered aquarium, in most cases, the subjects jumped onto it without stimulation; otherwise, the subject's escape reaction was provoked by short blasts of air. During each experimental session, the subject was made to jump three times. The whole jumping process of each subject was filmed with a high-speed video camera (MotionPro X3, Integrated Design Tools, IDT) at 1000 frames per second (fps) using image acquisition software from Motion Studio (IDT). Graph paper was used for scale to calibrate jump lengths. High-speed images of spider jumping were analysed using motion analysis software TEMA v. 2.6 (Image Systems). The position of the tip of the cephalothorax (head), the cephalothorax–abdomen joint or pedicel (middle) and the end of the abdomen (tail) were tracked for each subject (figure 1*b*).

The trajectory of the spider's middle, assumed to be its CoM, throughout a jump was smoothed by a cubic polynomial using Origin v. 8.5 (OriginLab Corporation) to reduce tracking error. Velocity $v(t)$ and acceleration $a(t)$ were then calculated as the first and second derivatives, respectively, of the position function. The body orientation of each spider was analysed as follows: the directions of the cephalothorax and abdomen were their angles relative to the horizontal plane (θ_C and θ_A, respectively), and the cephalothorax–abdomen angle bisector (θ_B) was used to represent overall body direction. Hence, head orientation can be quantified as θ_C and body posture as the cephalothorax–abdomen angle ($\theta_{A-C} = \theta_A - \theta_C$; figure 1*b*). Before take-off, the spider attached a

Table 1. Body size, jumping kinematics and mechanical energy during salticid jumping (mean ± s.d.). BM, body mass; BL, body length; θ_i, direction of take-off velocity; v_i, v_f: velocity at take-off and landing, respectively; D, distance travelled; T_{air}, T_{land}: duration of the aerial phase and landing phase, respectively; Δv, change of velocity between take-off and landing. Subscripts X and Z denote horizontal and vertical directions, respectively. E_i, mechanical energy at take-off; ΔE, change of mechanical energy between take-off and landing. Mechanical energy (E) was calculated as the sum of the kinetic energy and potential energy, and the latter was set to zero for take-off.

	BM (mg) BL (mm)	θ_i (°)	v_i v_f (m s^{-1})	v_{iX} v_{iZ} (m s^{-1})	D_X D_Z (cm)	T_{air} T_{land} (ms)	Δv_X Δv_Z (m s^{-1})	E_i (µJ)	ΔE (µJ)	$\Delta E/E_i$ (%)
silk	19.95 ± 4.71	11.4 ± 5.2	0.99 ± 0.13	0.96 ± 0.14	9.36 ± 1.43	116 ± 13	-0.38 ± 0.07	10 ± 4	-7 ± 2	76 ± 18
($n = 15$)	6.1 ± 0.3		1.0 ± 0.09	0.19 ± 0.08	-3.81 ± 0.31	10 ± 2	-1.0 ± 0.12			
non-silk	21.14 ± 2.83	5.0 ± 10.0	0.94 ± 0.07	0.92 ± 0.07	8.91 ± 2.04	101 ± 20	-0.08 ± 0.05	9 ± 2	-3 ± 0.8	33 ± 11
($n = 4$)	6.0 ± 0.2		1.2 ± 0.04	0.08 ± 0.17	-3.89 ± 0.17	51 ± 29	-0.93 ± 0.18			
p*								0.762	0.002	<0.001

*p-Values of two-tailed t-test on calculated mechanical energy of normal and non-silk subjects. Statistical results for other comparisons are presented in table 3 and electronic supplementary material, tables S1, S2 and S4.

Table 2. Body orientation and its change at different stages of salticid jumping (mean ± s.d.). Statistical results for comparisons between the two groups are presented in table 3 and electronic supplementary material, table S3. θ_C, θ_{A-C} denote cephalothorax and body angles representing the body orientation as shown in figure 1*b*. $\Delta\theta_C$, $\Delta\theta_{A-C}$ denote change of cephalothorax and body angles.

	at take-off at landing		change in air change during landing	
	θ_C (°)	θ_{A-C} (°)	$\Delta\theta_C$ (°)	$\Delta\theta_{A-C}$ (°)
silk ($n = 15$)	−8.4 ± 4.7	179.5 ± 4.9	17.2 ± 11.0	−32.1 ± 8.8
	8.8 ± 11.1	147.4 ± 6.6	−15.2 ± 8.2	23.9 ± 15.9
non-silk ($n = 4$)	−9.4 ± 3.8	182.7 ± 4.6	66.8 ± 21.6	−5.8 ± 10.9
	57.4 ± 18.9	176.9 ± 13.7	−49.6 ± 19.5	−1.2 ± 17.7

dragline silk to the substrate, and the location of the attachment point could be identified from the high-speed image at the moment when the subject contacted its tail to the ground. Silk production and attachment were confirmed by checking the substrate after each jumping trial. The silk stayed straight throughout a jump (as seen in some frames of electronic supplementary material, movie S1), and therefore we could calculate the silk angle (θ_S) and the silk–abdomen angle (θ_{S-A}) from known silk–attachment positions to obtain the association between silk and spider (figure 1*c*).

2.3. Kinetics of spider jumping

During jumping, the spider's acceleration (a) is determined by the net force it experienced, which is composed of gravity (mg), drag from the air (F_D) and silk force (F_S)

$$F = mg + F_S + F_D = ma(t), \tag{2.1}$$

where m is the spider's mass and g is gravitational acceleration. Therefore, the instantaneous F_S can be calculated with known $a(t)$, mg and F_D. Given an air density (ρ) of 1 kg m^{-3} and viscosity (μ) of 18×10^{-6} Pa s, a spider with length $l = 0.6$ cm jumping at velocity $v = 0.6$–1 m s^{-1} would have a Reynolds number ($Re = \rho l v/\mu$) of 200–400. For this range of Re, pressure drag (F_D) can be estimated as follows

$$F_D = \frac{1}{2} C_d \rho A v^2, \tag{2.2}$$

where C_d is the drag coefficient, A is the projection area facing the direction of the spider's motion and v is the instantaneous velocity of the spider's CoM calculated as the first derivative of the fitted position function. The direction of drag is opposite to that of CoM's velocity (figure 1*c*).

The C_d of a sphere based on the frontal area is 0.5; but for $Re < 1000$, C_d is calculated as follows [35]

$$C_d = \frac{24}{Re} + \frac{6}{1 + Re^{1/2}} + 0.4. \tag{2.3}$$

Hence for $Re \sim 200$–400, C_d for a sphere should be 0.75–0.92.

Because non-silk salticids were subjected only to gravity and drag during jumping, we could determine the most appropriate C_d by comparing their velocity change in the horizontal direction ($\Delta v_X(t)$) to what is predicted using $C_d = 0.5$–2.0. This range covered C_d equal to 1, which has previously been used for some jumping insects [36]. The C_d leading to the best prediction was then used to calculate the drag experienced by normal spiders. Reference area A is empirically defined as the frontal projection area (FPA) of the spider in the moving direction, and was calculated as the area projected onto the plane normal to the instantaneous velocity vector (figure 1*c*). Because body postures changed throughout the aerial phase, we treated each body segment (cephalothorax and abdomen) separately, approximated its projection as an ellipse and calculated FPA using segment length, width and angle relative to the projection plane (figure 1*c*). The projected area of the body's transverse plane was also included. The maximum FPA of eight legs (measured from top view) was comparable with that of the body. We assumed that the legs and body had a similar projected area because they usually had a similar orientation during jumping.

2.4. Estimating drag and silk force

We treated horizontal (x-direction) and vertical (z-direction) motions separately in our analysis. To demonstrate the relative contribution of dragline silk on spider motion, we first compared the kinematic variable (velocity change in x-direction, Δv_X) between empirical data from normal spiders to predictions for the non-silk condition

$$\Delta v_X(t) = v_X(t) - v_{X0} = a_X(t) \cdot t, \tag{2.4}$$

where v_{X0} is the initial velocity. Forces acting on the subject, as described in equation (2.1), can be decomposed into x- and z-directions

$$\left.\begin{aligned} F_X &= F_{DX} + F_{SX} = ma_X(t) \\ \text{and} \quad F_Z &= mg + F_{DZ} + F_{SZ} = ma_Z(t), \end{aligned}\right\} \tag{2.5}$$

where $a_X(t)$ and $a_Z(t)$ are the instantaneous accelerations in the x- and z-directions, calculated as the second derivative of the corresponding position function fitting the original data. Drag and silk forces in the x- and z-directions can be calculated as

$$\left.\begin{aligned} F_{DX} &= F_D \cdot \cos\theta_D \text{ and } F_{SX} = F_S \cdot \cos\theta_S \\ \text{and} \quad F_{DZ} &= F_D \cdot \sin\theta_D \text{ and } F_{SZ} = F_S \cdot \sin\theta_S, \end{aligned}\right\} \tag{2.6}$$

where drag, silk forces and directions are shown in figure 1*c*. Therefore, the prediction of $\Delta v_X(t)$ for the non-silk condition can be made (equation (2.4)) using acceleration calculated from equations (2.5) and (2.6) with $F_{SX} = 0$

$$a_X(t) = \frac{F_{DX}}{m} = \frac{F_D \cdot \cos\theta_D}{m}, \tag{2.7}$$

where the drag force F_D can be calculated using equation (2.2) and C_d determined as described in section 2.3.

Finally, the instantaneous silk force F_{SX} can be calculated using equation (2.5) with known mass, empirically obtained acceleration $a_X(t)$ and calculated drag F_{DX}. F_S was further calculated with known silk direction (equation (2.6) and figure 1*c*).

2.5. Statistical analyses

The mean and standard deviation of jumping kinematics, body orientation and mechanical energy were calculated to assess the jumping performances of normal and non-silk subjects (for variables, see tables 1 and 2). Besides comparing body size and

take-off velocity (see §2.1), we also performed statistical analyses to compare the aforementioned variables between the two groups. We used SAS/STAT software, v. 9.3 of the SAS System for WINDOWS [37] and R [38] with package 'nlme' [39], and set $p < 0.05$ as the criterion for significance.

To examine whether silk has effects on the aerial phase of jumping, we conducted separate comparisons for translational and rotational variables using two-way nested multivariate analysis of covariance (MANCOVA), with silk condition (value is 1 for silk, 0 is for non-silk) as a fixed factor and individual (nested within silk condition) as a random factor. We used transformed dependent variables if the distribution of residuals of a MANOVA/MANCOVA/GLMM was significantly non-normal. In the MANCOVA test for the translational variables of flight duration (T_{air}) and velocity changes (Δv_X, horizontal; Δv_Z, vertical), we considered the following covariates: body size (BM, BL), initial velocity (v_i), jumping distance in two directions (D_X, D_Z), take-off angle (θ_i) and modifications of these variables (see electronic supplementary material, table S2). In the MANCOVA test for the rotational variables of body orientation at landing (landing θ_C and landing θ_{A-C}), we considered two extra rotational covariates (take-off θ_C and take-off θ_{A-C}; electronic supplementary material, table S3). If the overall effect of silk is significant in the MANCOVA test, then we fitted the dependent variable to a GLMM and selected the best model by stepwise selection with Akaike information criterion (AIC).

Finally, we examined silk's effect on landing duration (T_{land}) using a GLMM, also setting silk condition as a fixed factor and individual as a random factor. Covariates for this model included the body size (BM, BL), landing velocity (v_f), jumping distance (D_X, D_Z) and body orientation at landing (landing θ_C and landing θ_{A-C}; figure 2*a* and electronic supplementary material, movie S4). We selected the best model by stepwise selection with AIC.

3. Results and discussion

3.1. Silk's effects on jumping kinematics and body orientation

To discern dragline silk's functional significance as a safety line and in-air stabilizer, we first analysed the kinematics of 57 jumps from 19 female jumping spiders (*H. adansoni*), among which four subjects stopped producing silk before experiments. Table 1 summarizes the results of jumping performance, velocity changes and mechanical energy dissipation. Table 2 summarizes head orientation and body angles at take-off and landing, as well as changes that occurred during aerial and landing phases. Because no measurable difference was found between normal and non-silk spiders in body size, take-off velocity and mechanical energy (§2.1; table 1 and electronic supplementary material, table S1 and figure S1), observed differences in jumping mechanics could be attributed to the existence of dragline silk. Table 1 suggests that despite similar jumping performance (distance D_X and height D_Z), normal spiders stayed in the air longer (T_{air}) and decelerated more horizontally (Δv_X) than those without silk. Equipped with dragline silk as a safety line, normal spiders lost significantly greater mechanical energy, accounting for 76% of the original mechanical energy, which is significantly greater than the 33% that was lost by non-silks (table 1).

We examined the extent that silk affects spider jumping during aerial and landing phases by conducting separate comparisons of two-way nested MANCOVA using various sets of covariates. Results suggest a significant overall effect of silk on various translational (T_{air}, Δv_X and Δv_Z; $\Lambda_{Wilks} = 0.4927$, $F_{3,15} = 5.15$, $p = 0.0120$) and rotational variables (landing θ_C and landing θ_{A-C}; $\Lambda_{Wilks} = 0.3533$, $F_{2,16} = 14.64$, $p = 0.0002$) for the aerial phase of jumping. We further constructed GLMMs to discern silk's contribution to them (T_{air}, ΔV_X and ΔV_Z in electronic supplementary material, table S2; landing θ_C and landing θ_{A-C} in electronic supplementary material, table S3). For the landing phase, the model suggested a significant effect of silk on landing duration (T_{land}) ($T_{15} = -2.3367$, $p = 0.0337$; electronic supplementary material, table S4). Table 3 summarizes the coefficients of silk condition for each kinematic-dependent variable in its corresponding GLMM and the differences in empirical data of the two groups (tables 1 and 2). Because the value for silk condition was set to be 1 for silk and 0 for non-silk, each coefficient represents a suggested difference that silk made for that dependent variable by the model, which took the effects of covariates into account.

Our study reveals that a jumping spider with dragline silk has a more dynamically stable body posture and smoother landing (see electronic supplementary material, movies S1–S3). After take-off, increasing body angles in spiders of either group imply initial rearward torque (figure 2*a*,*b*), consistent with other salticids reported previously [21,22]. By contrast, wandering spiders pitch forward, probably because of the different relative position of CoM and leg extension mechanisms [40,41]. To counteract this initial pitch moment and prevent in-air rotation, previous studies suggest that spiders could adjust leg movement or use silk to reverse body orientation towards the ends of long jumps [21,22,40]. But here we show that normal salticids underwent multiple pitch reversals (see electronic supplementary material, figure S2*a* and movie S4) to land at shallower body angles (figures 2*c* and 3 and table 2). The GLMM suggests that non-silk spiders would land with a head angle (θ_C) $40.97 \pm 7.08^\circ$ greater than normal ones (table 3 and electronic supplementary material, table S3). Among 44 jumps from 15 normal subjects throughout the aerial phase ($T_{air} = 116 \pm 13$ ms), six jumps underwent three pitch reversals, 23 jumps had two reversals, 13 jumps had one reversal and two jumps had none. For jumps with two or more pitch reversals, the first occurred at 32 ± 8 ms after take-off (approx. $31 \pm 11\%$ T_{air}) and the second at 85 ± 21 ms after take-off (approx. $72 \pm 14\%$ T_{air}).

By contrast, non-silk spiders underwent greater rearward pitch (in-air $\Delta\theta_C$) and landed more upright with greater variation in orientation (landing θ_C), implying less predictable body postures (figures 2*b*,*c* and 3; tables 2 and 3; electronic supplementary material, table S3 and movie S5). Consequently, they required greater forward pitch to complete a landing ($\Delta\theta_C$ during landing) and might even slip or tumble due to inappropriate foot–ground contact (figure 3*b*,*c*). Compared with normal spiders, the bodies of non-silks hit the ground much earlier and hence were subject to greater impact forces. Although the spider is less likely to be injured by impact owing to tumbling [42], a non-silk spider landing unstably needs more time to complete a landing (T_{land}) than a normal spider (51 ± 29 versus 10 ± 2 ms) before proceeding to capture prey (figure 3 and table 1). The GLMM suggests that the decrease of T_{land} due to silk alone was 13.11 ± 5.61 (table 3 and electronic supplementary material, table S4). The other factor with significant effect on T_{land} was θ_C at landing (see electronic supplementary material, table S4). With a coefficient of approximately 0.3, a difference in landing θ_C between the two groups (approx. 50° in table 2) would lead to T_{land} being approximately 15 ms longer in non-silk

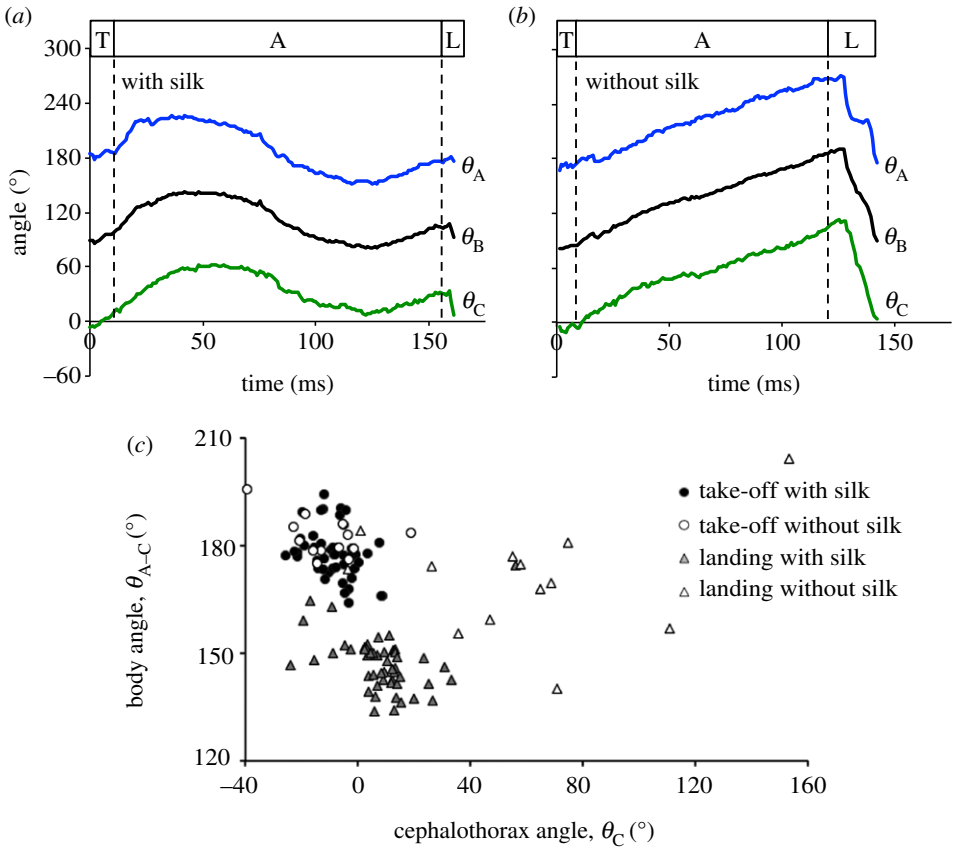

Figure 2. Body orientation during spider jumping. (*a*,*b*) Change of body orientation, θ_A, θ_B and θ_C as shown in figure 1*c*, in a normal and a non-silk spider during the take-off (T), aerial (A) and landing (L) phases. Animation of these two events is shown in electronic supplementary material, movies S4 and S5. (*c*) Relationship between spider's body angles (θ_{A-C}) and head orientation (θ_C) at take-off (filled circles, open circles) and landing (filled triangles, open triangles; solid symbols denote 44 trials from 15 normal subjects, and open symbols denote 13 trials from four non-silk subjects). (Online version in colour.)

Table 3. Coefficients of silk conditions for various kinematic variables fitted by a general linear mixed model (GLMM) after AIC model selection. Silk (yes, 1; no, 0) was considered a fixed factor and individual (nested within silk condition) as a random factor. Each set of model used different combinations of covariates. The differences in empirical data of the two groups are also presented for comparison.

	GLMM					
	dependent variables	covariates[a]	coefficient ± s.e. of 'silk' factor	*p*	reference	empirical difference (silk − non-silk)
1	V_i (m s^{-1})	a, b	0.038 ± 0.038	0.3387	electronic supplementary material, table S1	0.05
2	T_{air} (ms)	a, b, c, e, f, g	6.324 ± 1.897	0.0039	electronic supplementary material, table S2	15.8
	ΔV_X (m s^{-1})		−0.257 ± 0.040	<0.0001		−0.30
	ΔV_Z (m s^{-1})		0.038 ± 0.014	0.0132		−0.07
3	landing θ_C (°)	a, b, c, e, f, g, h, i	−40.97 ± 7.08	<0.0000	electronic supplementary material, table S2	−48.6
	landing θ_{A-C} (°)		−21.85 ± 3.59	<0.0000		−29.5
4	T_{land} (ms)	a, b, d, e, f, j, k	−13.11 ± 5.61	0.0337	electronic supplementary material, table S4	−40.3

[a]Covariates: (a) BM; (b) BL; (c) v_i; (d) v_f; (e) D_X; (f) D_Z; (g) $\theta_i - 45°$; (h) θ_C at take-off; (i) θ_{A-C} at take-off; (j) θ_C at landing; (k) θ_{A-C} at landing. When variables (a–f) were made covariates, their squares were also considered in the model.

subjects. These results suggest that dragline silk can function as a body stabilizer to prepare salticids for a predictable, optimal landing posture, and hence is critical for these agile and efficient hunters.

3.2. Relative contribution of drag and silk force

During jumping, the spider experiences mg, F_D and F_S (equation (2.1). We discerned the relative contribution of dragline silk on spider motion by comparing empirical

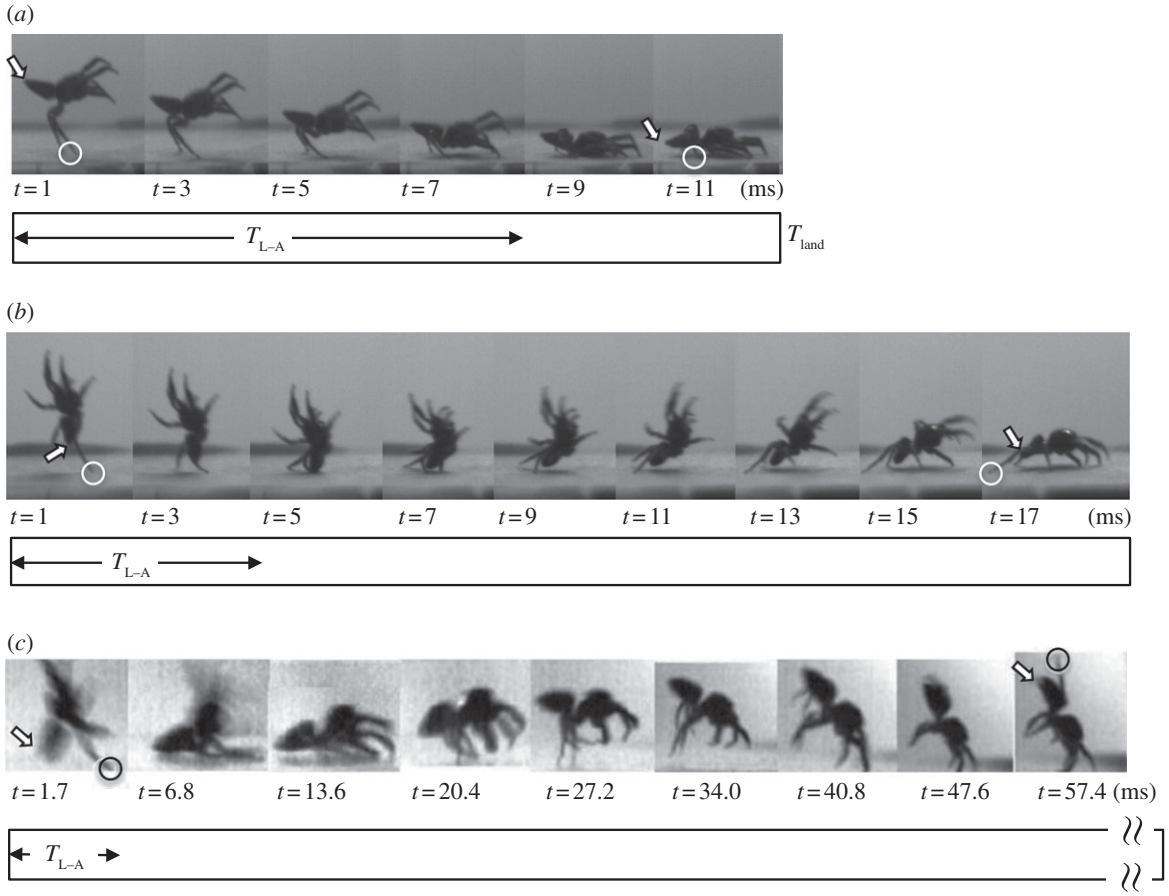

Figure 3. Landing motions of normal and non-silk jumping spiders, recorded using a high-speed video camera (*a*,*b* filmed at 1000 fps; *c* filmed at 600 fps). (*a*) The spider with silk kept a stable body orientation and leg–ground contact throughout the landing phase (with duration T_{land}). (*b*,*c*) Non-silk spiders landing upright hit the ground with their abdomens shortly after the leg contact (shorter T_{L-A}), and underwent faster forward rotation. They can even slip and tumble due to unfavourable initial leg–ground contact (as shown in (*c*), three out of 13 events), which defers the completion of landing (longer T_{land}). The arrow and circle in (*a*,*b*) indicate the tip of the abdomen and the leg, respectively, at the beginning and the end of the landing phase.

kinematic data to what was predicted for the non-silk condition. Hence, the deviation of empirical data from predicted values shows the effect of silk force. We treated horizontal (*x*-direction) and vertical (*z*-direction) motions separately in our analyses. In the *x*-direction, acceleration $a_X(t)$ was $-0.7 \pm 0.6\ \mathrm{m\ s^{-2}}$ for non-silk ($n = 4$) and $-3.2 \pm 0.7\ \mathrm{m\ s^{-2}}$ for normal spiders ($n = 15$). In the *z*-direction, $a_Z(t)$ was $-9.3 \pm 0.5\ \mathrm{m\ s^{-2}}$ for non-silk and $-8.5 \pm 0.3\ \mathrm{m\ s^{-2}}$ for normal spiders, suggesting that drag alone contributed a force of approximately 5% of body weight (BW), whereas silk contributed an additional force of approximately 8% BW. Therefore, the vertical motion of spiders was predominantly determined by gravity, and the effect of drag or silk was negligible in the analyses.

In contrast to previous notions interpreted from jumping trajectories [22], our results suggest that drag cannot be neglected especially in determining horizontal motion. Even without silk, velocity change deviated from the ideal condition of no drag (figure 4*a*), and approximately $33 \pm 11\%$ of a spider's initial mechanical energy was dissipated (table 1). To estimate C_d, we compared the empirical results of Δv_X of non-silk spiders ($-0.08 \pm 0.05\ \mathrm{m\ s^{-1}}$; $n = 4$; table 1) with those predicted using $C_d = 0.5$–2.0 (figure 4*a*). Empirical data from non-silk spiders suggest that Δv_X is best estimated using $C_d \sim 1.5$ ($\Delta v_X = -0.08 \pm 0.03\ \mathrm{m\ s^{-1}}$), which is greater than suggested for a sphere at a similar range of *Re* ($C_d = 0.75$–0.92 calculated using equation (2.3), for $Re = 200$–400). Hence, assuming that jumping spiders (or insects of similar size) are spherical in shape will underestimate the drag experienced. Figure 4*a* suggests that a different C_d yielded the best prediction of Δv_X at each moment, presumably owing to varying body shapes throughout a jump.

Using the same criteria to calculate drag for normal spiders allowed us to demonstrate silk's relative effects on spider motion, as indicated by the deviation of empirical data from predictions (figure 4*b*). To quantify the instantaneous F_S, we first considered the horizontal direction (equation (2.5)) to estimate the *x*-component of silk force (F_{SX}) from acceleration $a_X(t)$ and F_{DX}. The latter was calculated from F_D and its direction (equation (2.6) and figure 1*c*). F_D for each event was calculated using $C_d = 1.5$, the FPA facing the direction of the spider's motion and the instantaneous velocity of the subject's CoM (equation (2.2)). Finally, we used the known silk direction θ_S to calculate F_S (equation (2.6) and figure 1*c*). Our results suggest that the mean F_S is $50.4 \pm 11.1\ \mu\mathrm{N}$ ($26 \pm 4\%$ BW; $n = 15$) throughout the aerial phase.

The relative contribution of drag and silk forces exerted on a subject varied with time (figure 4*c*). Silk force was dominant and kept at approximately 80% of total resistant force during the first half of jumping; however, during the last quarter of jumping, silk's influence declined to

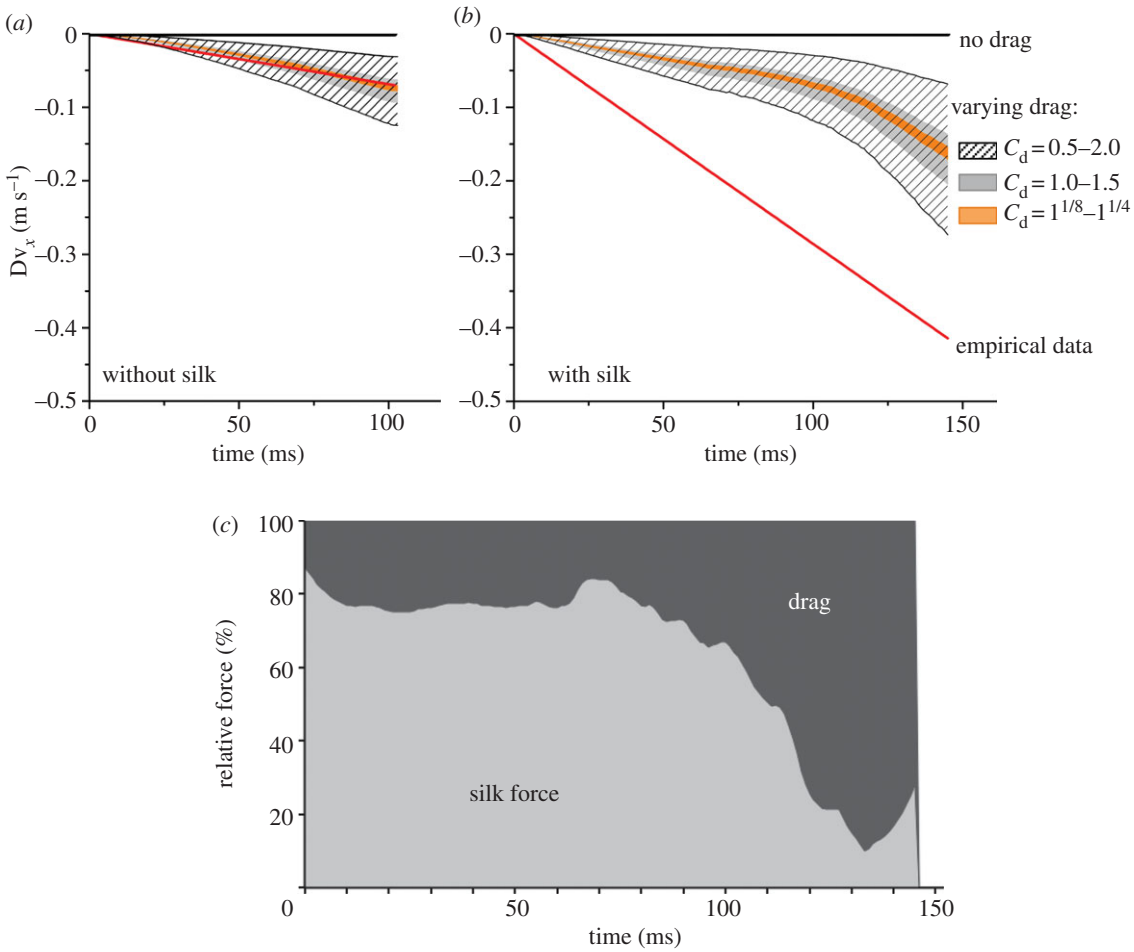

Figure 4. Velocity change and external forces throughout a spider's jump. (*a*,*b*) Velocity change in the *x*-direction is based on empirical data (red lines) and predictions using drag coefficients $C_d = 0.5-2.0$ in normal and non-silk spiders. Without drag, the horizontal velocity would not change (i.e. $\Delta v_X = 0$), as indicated by the horizontal lines. For non-silk subjects, on average, a prediction for total Δv_X calculated using $C_d \sim 1.5$ yields the best fit to the empirical data ($n = 4$; the best fit in this case occurred at $C_d \sim 1.125$). In normal spiders, deviation of empirical data from predicted values suggests the effect of silk force. (*c*) The relative contribution of drag and silk to the total force exerted on a normal subject throughout a jump (same subject as in (*b*)).

approximately 20%, and resistance was dominated by drag. For the normal subject reported in figure 4*b*,*c*, 67% of the initial mechanical energy was dissipated by braking, in which drag and silk friction contributed comparably (32% and 35%, respectively).

3.3. In-air stability control with adjustable silk force

Temporal patterns of changes in body and silk angles (θ_A and θ_{S-A}) and resistant forces (F_D and F_S) reveal how dragline silk is used to adjust body orientation and stabilize jumping (figure 5). After take-off, the subject elevated its head with θ_A increasing from approximately 180° to 220° owing to the initial rearward pitch moment, but the silk–abdomen angle θ_{S-A} decreased to approximately 140° until the first pitch reversal (forward rotation) occurred about 10 ms later, as opposed to being towards the end of a jump as previously reported [22]. Analyses suggested that the maximum silk force $F_S \sim 79.6 \pm 15.8$ µN (42 ± 11% BW; $n = 15$) occurred at take-off and remained almost constant until the abdomen angle θ_A returned to approximately 180° (approx. 70 ms after take-off in figure 5). During this time, F_S acting on the tail provided a moment $M_S = F_S \cdot \sin \theta_{S-A}$, maximum at 60.3 ± 28.4 nN m, to rotate the abdomen forward about the pivot (middle) of the body (figures 1*c* and 5). The abdomen continued to pitch forward below 180° but with less amplitude than before, whereas the slightly decreased F_S began to provide a moment with the opposite direction to slow down forward pitch until the second reversal (approx. 107 ms in figure 5). Subsequently, the subject pitched rearward again to approach horizontal towards the end of the aerial phase, during which F_S decreased drastically and provided little moment on the tail. During the stage of last reversal, drag F_D instead increased to decelerate the subject (figure 4*c*). Such varying of silk force is presumably controlled by the valve of the spinning system [34].

Throughout the aerial phase, θ_A and θ_{S-A} fluctuated about 180° out of phase for multiple cycles (figure 5), revealing the first evidence that dragline silk provides a counteracting torque for dynamic pitch control during spider jumping. After take-off, a constant and greater silk force controls the first pitch reversal and diminishes fluctuations in later body rotations. Decreasing silk force, and hence moment, towards the end of the aerial phase could prevent the body from further rotation (pitch reversal). Consequently, silk that is almost aligned in parallel to the abdomen could be more effective in braking.

In a jumping spider, silk force could result from material extension or an internal brake [33]. The latter might be served by the valve of the spinning system clamping onto

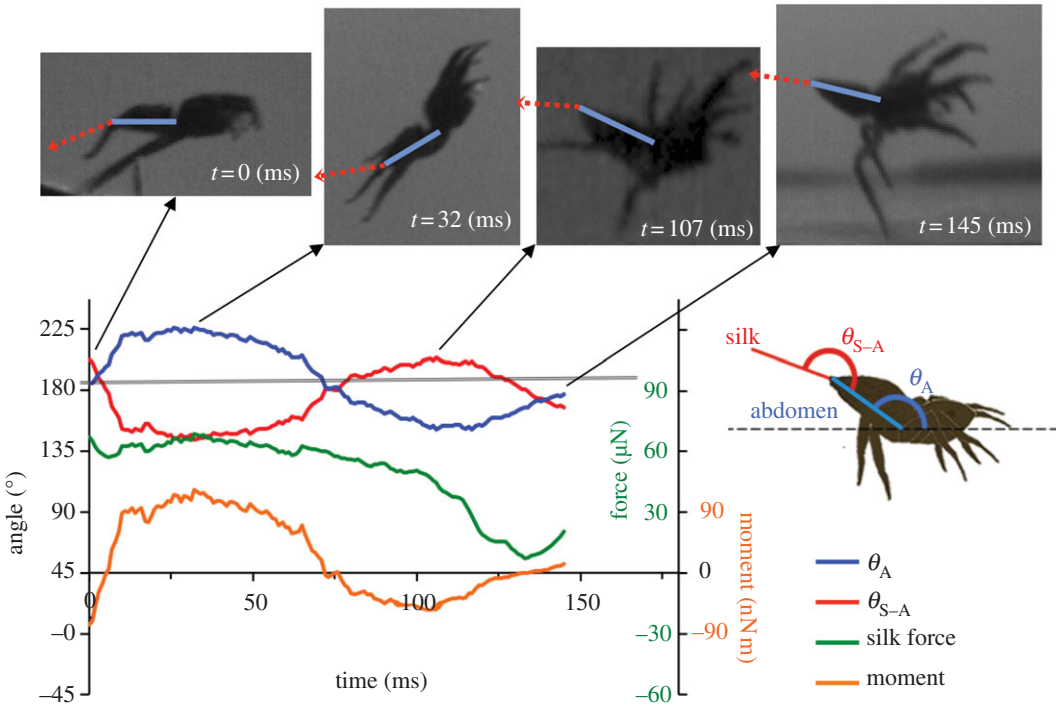

Figure 5. Body orientation, silk orientation, silk force and moment throughout a spider's jump. Abdomen angle (θ_A) and silk–abdomen angle (θ_{S-A}) fluctuated about 180° and were out of phase during the course of jumping. The direction of the abdomen and silk is shown on the high-speed images at take-off, pitch reversals (at approx. 32 ms and approx. 107 ms after take-off) and the end of the aerial phase.

newly produced silk as proposed for orb-weaving spiders [32,34]. Silk force exerted on a descending orb-weaving spider ranges between 0.1 from silk spooling and 2.2 BW from a fully activated internal brake [33]. Although our estimated silk force of 10–80 μN (approx. 0.05–0.4 BW), presumably owing to varying activation of the internal brake, cannot fully stop a jumping spider, it effectively decreased its landing velocity and reversed its body rotation (figures 2, 4 and 5 and tables 2 and 3).

Under complete braking, dragline silk is held tightly and subjected to external forces from the spider's momentum change during jumping. The efficiency of such a safety line can be evaluated using safety factor (SF), which is a ratio of a material's loading capacity to the actual load experienced. From a reported strength (1.19 GPa) [32] and measured cross-sectional areas of dragline silk of two threads (514 ± 73.2 nm each in diameter measured from SEM images, $n = 14$; Chen & Chi, 2010, unpublished data), the maximum force that silk could sustain is about 490 μN. To stop our subjects having a mass of 20 ± 5 mg jumping at a mean acceleration of 9.18 ± 0.84 m s^{-2}, the force exerted on the silk would be 180 ± 44 μN, about 0.9 ± 0.2 BW ($n = 15$). Therefore, the average SF of dragline silk during jumping is 2.7. At a force that is twice the mean, SF would decrease to about 1.4, similar to what was reported previously for dragline silks from orb-weaving spiders [32]. Despite the fact that reeling speed during jumping (up to 1000 mm s^{-1}) is an order of magnitude greater than the maximum used in forced silking (0.1–100 mm s^{-1}) or natural descending, the mean stress that we estimated on silk fibres during jumping (434 ± 105 MPa) is similar to the range of stress reported for forcibly silked fibres from *Argiope trifasciata* at various speeds [43,44]. During salticid jumping, both the mean silking force and silk diameter were about an order of magnitude smaller than what was measured during the forced silking from the orb-web spiders.

4. Conclusions

Dragline silks, renowned for their superb properties, provide multifaceted functions that shape spider ecology and evolution. Here, we demonstrate that the dragline silk of salticids not only works as a safety line for deceleration but also, more importantly, works as a body stabilizer throughout the jump. With acute vision, remarkable predatory strategies and jumping ability, dynamic stability further enhances prey-capture efficiency in hunters such as salticids. In addition to using the inertia of swinging appendages and aerodynamic forces from flapping wings, we propose herein a newly discovered third mechanism for in-air stability control found in nature. Dragline silk, in accordance with varying adjustable forces for pitch reversals, can stabilize the spider throughout a jump. Counteracting torque from adjustable silk tension provides biological inspiration for future manoeuvrable robot designs.

Acknowledgements. We thank M.-C. Shih, M.-H. Wu, I.-M. Tso, E.-C. Yang, J.-R. Roan, H.-Y. Tzeng, H.-D. Huang and the Shih-Roan-Chi Joint Group for assistance and discussion, and the anonymous referees for helpful comments and suggestions.

Funding statement. This study was supported by the National Science Council (NSC) of Taiwan to K.-J.C. (grant no. 96-2112-M-005-002-MY3). An early stage of this study was conducted when Y.-K.C. participated in the NSC High Scope Programme and the National Taiwan Science Education Centre (NTSEC) Young Scientists Development Programme.

References

1. Alexander RM. 2006 *Principles of animal locomotion*. Princeton, NJ: Princeton University Press.
2. Bennet-Clark HC, Lucey ECA. 1967 The jump of the flea: a study of the energetics and a model of the mechanism. *J. Exp. Biol.* **47**, 59–76.
3. Alexander RM. 1995 Leg design and jumping technique for humans, other vertebrates and insects. *Phil. Trans. R. Soc. Lond. B* **347**, 235–248. (doi:10.1098/rstb.1995.0024)
4. Gronenberg W. 1996 Fast actions in small animals: springs and click mechanisms. *J. Comp. Physiol. A* **178**, 727–734. (doi:10.1007/bf00225821)
5. Burrows M. 2003 Froghopper insects leap to new heights. *Nature* **424**, 509. (doi:10.1038/424509a)
6. Burrows M. 2006 Jumping performance of froghopper insects. *J. Exp. Biol.* **209**, 4607–4621. (doi:10.1242/jeb.02539)
7. Cofer D, Cymbalyuk G, Heitler WJ, Edwards DH. 2010 Control of tumbling during the locust jump. *J. Exp. Biol.* **213**, 3378–3387. (doi:10.1242/jeb.046367)
8. Emerson SB. 1985 Jumping and leaping. In *Functional vertebrate morphology* (eds M Hildebrand, DM Bramble, KF Liem, DB Wake), pp. 58–72. Cambridge, MA: Harvard University Press.
9. Jusufi A, Goldman DI, Revzen S, Full RJ. 2008 Active tails enhance arboreal acrobatics in geckos. *Proc. Natl Acad. Sci. USA* **105**, 4215–4219. (doi:10.1073/pnas.0711944105)
10. Gillis GB, Bonvini LA, Irschick DJ. 2009 Losing stability: tail loss and jumping in the arboreal lizard *Anolis carolinensis*. *J. Exp. Biol.* **212**, 604–609. (doi:10.1242/jeb.024349)
11. Jusufi A, Kawano DT, Libby T, Full RJ. 2010 Righting and turning in mid-air using appendage inertia: reptile tails, analytical models and bio-inspired robots. *Bioinsp. Biomim.* **5**, 045001. (doi:10.1088/1748-3182/5/4/045001)
12. Libby T, Moore TY, Chang-Siu E, Li D, Cohen DJ, Jusufi A, Full RJ. 2012 Tail-assisted pitch control in lizards, robots and dinosaurs. *Nature* **481**, 181–184. (doi:10.1038/nature10710)
13. Nguyen Q-V, Park HC. 2012 Design and demonstration of a locust-like jumping mechanism for small-scale robots. *J. Bionic. Eng.* **9**, 271–281. (doi:10.1016/S1672-6529(11)60121-2)
14. Foelix RF. 1996 *Biology of spiders*, 2nd edn. New York, NY: Oxford University Press.
15. Hill D. 1979 Orientation by jumping spiders of the genus *Phidippus* (Araneae: Salticidae) during the pursuit of prey. *Behav. Ecol. Sociobiol.* **5**, 301–322. (doi:10.1007/BF00293678)
16. Richman DB, Jackson RR. 1992 A review of the ethology of jumping spiders (Araneae, Salticidae). *Bull. Br. Arachnol. Soc.* **9**, 33–37.
17. Vollrath F, Selden P. 2007 The role of behavior in the evolution of spiders, silks, and webs. *Annu. Rev. Ecol. Evol. Syst.* **38**, 819–846. (doi:10.1146/annurev.ecolsys.37.091305.110221)
18. Osaki S. 1996 Spider silk as mechanical lifeline. *Nature* **384**, 419. (doi:10.1038/384419a0)
19. Blackledge TA. 2012 Spider silk: a brief review and prospectus on research linking biomechanics and ecology in draglines and orb webs. *J. Arachnol.* **40**, 1–12. (doi:10.1636/m11-67.1)
20. Parry DA, Brown RHJ. 1959 The hydraulic mechanism of the spider leg. *J. Exp. Biol.* **36**, 423–433.
21. Parry DA, Brown RHJ. 1959 The jumping mechanism of salticid spiders. *J. Exp. Biol.* **36**, 654–664.
22. Hill DE. 2006 Targeted jumps by salticid spiders (Araneae, Salticidae, *Phidippus*), *ver. 9, 1–28*. See http://www.peckhamia.com/epublications.html.
23. Vollrath F. 1999 Biology of spider silk. *Int. J. Biol. Macromol.* **24**, 81–88. (doi:10.1016/S0141-8130(98)00076-2)
24. Suter RB. 1991 Ballooning in spiders: results of wind tunnel experiments. *Ethol. Ecol. Evol.* **3**, 13–25. (doi:10.1080/08927014.1991.9525385)
25. Gorb SN, Barth FG. 1994 Locomotor behaviour during prey-capture of a fishing spider *Dolomedes plantarius* (Araneae: Araneidae): galloping and stopping. *J. Arachnol.* **22**, 89–93.
26. Agnarsson I, Kuntner M, Blackledge TA. 2010 Bioprospecting finds the toughest biological material: extraordinary silk from a giant riverine orb spider. *PLoS ONE* **5**, e11234. (doi:10.1371/journal.pone.0011234)
27. Gosline J, Lillie M, Carrington E, Guerette P, Ortlepp C, Savage K. 2002 Elastic proteins: biological roles and mechanical properties. *Phil. Trans. R. Soc. Lond. B* **357**, 121–132. (doi:10.1098/rstb.2001.1022)
28. Blackledge TA, Hayashi CY. 2006 Silken toolkits: biomechanics of silk fibers spun by the orb web spider *Argiope argentata* (Fabricius 1775). *J. Exp. Biol.* **209**, 2452–2461. (doi:10.1242/jeb.02275)
29. Guerette PA, Ginzinger DG, Weber BHF, Gosline JM. 1996 Silk properties determined by gland-specific expression of a spider fibroin gene family. *Science* **272**, 112–115. (doi:10.1126/science.272.5258.112)
30. Vollrath F, Knight DP. 2001 Liquid crystalline spinning of spider silk. *Nature* **410**, 541–548. (doi:10.1038/35069000)
31. Emile O, Floch AL, Vollrath F. 2006 Biopolymers: shape memory in spider draglines. *Nature* **440**, 621. (doi:10.1038/440621a)
32. Ortlepp CS, Gosline JM. 2008 The scaling of safety factor in spider draglines. *J. Exp. Biol.* **211**, 2832–2840. (doi:10.1242/jeb.014191)
33. Ortlepp CS, Gosline JM. 2004 Consequences of forced silking. *Biomacromolecules* **5**, 727–731. (doi:10.1021/bm034269x)
34. Vollrath F, Knight DP. 1999 Structure and function of the silk production pathway in the Spider *Nephila edulis*. *Int. J. Biol. Macromol.* **24**, 243–249. (doi:10.1016/s0141-8130(98)00095-6)
35. Vogel S. 2005 Living in a physical world II. The bio-ballistics of small projectiles. *J. Biosci.* **30**, 167–175. (doi:10.1007/BF02703696)
36. Bennet-Clark HC, Alder GM. 1979 The effect of air resistance on the jumping performance of insects. *J. Exp. Biol.* **82**, 105–121.
37. SAS Institute Inc. 2011 SAS/STAT 9.3 user's guide. Cary, NC: SAS Institute Inc.
38. R Core Team. 2013 *R: a language and environment for statistical computing*. Vienna, Austria: R Foundation for Statistical Computing.
39. Pinheiro J, Bates D, DebRoy S, Sarkar D, the R Development Core Team. 2013 *nlme: linear and nonlinear mixed effects models*. R package version 3.1-109. Vienna, Austria: R Foundation for Statistical Computing.
40. Weihmann T, Karner M, Full RJ, Blickhan R. 2010 Jumping kinematics in the wandering spider *Cupiennius salei*. *J. Comp. Physiol. A* **196**, 421–438. (doi:10.1007/s00359-010-0527-3)
41. Weihmann T, Gunther M, Blickhan R. 2012 Hydraulic leg extension is not necessarily the main drive in large spiders. *J. Exp. Biol.* **215**, 578–583. (doi:10.1242/jeb.054585)
42. Brandwood A. 1985 Mechanical properties and factors of safety of spider drag-lines. *J. Exp. Biol.* **116**, 141–151.
43. Pérez-Rigueiro J, Elices M, Plaza G, Real JI, Guinea GV. 2005 The effect of spinning forces on spider silk properties. *J. Exp. Biol.* **208**, 2633–2639. (doi:10.1242/jeb.01701)
44. Elices M, Guinea GV, Plaza GR, Real JI, Pérez-Rigueiro J. 2006 Example of microprocessing in a natural polymeric fiber: role of reeling stress in spider silk. *J. Mater. Res.* **21**, 1931–1938. (doi:10.1557/jmr.2006.0240)